Published in final edited form as:
Biomaterials. 2012 February ; 33(6): 1791–1800. doi:10.1016/j.biomaterials.2011.11.025.

The involvement of integrin β1 signaling in the migration and myofibroblastic differentiation of skin fibroblasts on anisotropic collagen-containing nanofibers

Chengyang Huang[1,*], **Xiaoling Fu**[1,*], **Jie Liu**[2], **Yanmei Qi**[2], **Shaohua Li**[2,#], and **Hongjun Wang**[1,#]

[1]Chemistry, Chemical Biology and Biomedical Engineering, Stevens Institute of Technology, Hoboken, NJ 07030, USA

[2]Department of Surgery, Robert Wood Johnson Medical School, New Brunswick, NJ 08903, USA

Abstract

Utilization of nanofibrous matrices for skin wound repair holds great promise due to their morphological and dimensional similarity to native extracellular matrix (ECM). It becomes highly desired to understand how various nanofibrous matrices regulate skin cell behaviors and intracellular signaling pathways, important to tuning the functionality of tissue-engineered skin grafts and affecting the wound healing process. In this study, the phenotypic expressions of normal human dermal fibroblasts (NHDFs) on collagen-containing nanofibrous matrices with either isotropic (*i.e.,* fibers collected randomly with no alignment) or anisotropic (*i.e.,* fibers collected with alignment) fiber organizations were studied by immunostaining, migration assay and molecular analyses. Results showed that both nanofibrous matrices supported the attachment and growth of NHDFs similarly, while showing different cell morphology with distinct variation in focal adhesion formation and distribution. Anisotropic nanofibers significantly triggered the integrin β1 signaling pathway in NHDFs as evidenced by an increase of active integrin β1 (130 kD mature form) and phosphorylation of focal adhesion kinase (FAK) at Tyr-397. Anisotropic matrices also promoted the migration of NHDFs along the fibers, while neutralization of the integrin β1 activity abolished this promotion. Moreover, the fibroblast-to-myofibroblast differentiation was greatly enhanced for the NHDFs cultured on anisotropic nanofibrous matrices over a period of 48 hours. Inhibition of cellular integrin β1 activity by neutralizing antibody eliminated this enhancement. These findings suggest the important role of integrin β1 signaling pathway in regulating the nanofiber-induced fibroblast phenotypic alteration and providing insightful understanding of the possible application of collagen-containing nanofibrous matrices for skin regeneration.

[#]Corresponding authors: S. Li, Department of Surgery, Robert Wood Johnson Medical School, 125 Paterson Street, New Brunswick, NJ 08903, USA. Tel: +1 732 235 6164; Fax: +1 732 235 8538;Shaohua.li@umdnj.edu.; H. Wang, Department of Chemistry, Chemical Biology and Biomedical Engineering, Stevens Institute of Technology, McLean Building Room 416, 1 Castle Point on Hudson, Hoboken, NJ 07030, USA. Tel: +1 201 216 5556; Fax: +1 201 216 8240; Hongjun.Wang@stevens.edu. .
[*]Equal contribution

Keywords

anisotropic nanofibers; normal human dermal fibroblasts; fibroblast-to-myofibroblast differentiation; integrin β1 signaling

1. Introduction

Tissue engineered skin grafts have proved to be effective in closing deep skin wounds despite their suboptimal structure, composition and function [1]. To better support and facilitate skin cells to form skin-like tissues, it is necessary for the temporary scaffolds not only to provide a surface for the cells to reside, but also to define a cell-friendly microenvironment that maximally recaptures the native extracellular matrix (ECM). In this regard, electrospun nanofibrous matrices characterized by ultrafine continuous nanoscaled fibers, high surface-to-volume ratio, high porosity and variable pore-size distribution have great potential to mimic the skin ECM in both morphology and composition [2, 3]. In recognition of the superiority of nanofibrous matrices, increasing efforts have been made to explore the possibility of creating tissue-engineered skin grafts using electrospun fibers. Clearly, nanofibrous matrices support the adhesion, spreading and proliferation of skin cells [4, 5].

Collagen fibrils, a major ECM component known for their mechanical contribution to skin integrity, provide an interactive 3D microenvironment to skin cells and regulate their behaviors via cell-matrix interactions. To better mimic skin ECM, electrospun collagen fibers have been fabricated, however, the rapid degradation and poor mechanical properties determine that either crosslinking or combination with other materials is necessary to obtain a stable scaffold. Electrospinning a blend solution of collagen and polycaprolactone (PCL), a biocompatible and biodegradable synthetic polyester, can yield rather stable nanofibers [6, 7]. Dermal fibroblasts showed preferred adhesion on such collagen-containing nanofibers, comparable to pure collagen fibers [5, 8]. In addition, it has been noted that organization of nanofibers in the matrices also affects the behaviors of dermal fibroblasts and adipose stromal cells [9-13], *e.g.*, fibroblasts cultured on aligned nanofibrous substrates became elongated with accelerated migration [12]. Although the exact mechanism is still unclear, it is believed that integrins are involved in the electrospun nanofiber-regulated cell adhesion [14], and the activation of various integrins during focal adhesion formation may influence cellular phenotype, which is critical to determine the functionality of tissue-engineered skin grafts *in vitro* and subsequently influence the quality of healed wounds upon *in vivo* grafting.

During normal wound healing the fibroblast-to-myofibroblast differentiation can facilitate wound closure by drawing the wound margins together, however, it would also result in scar formation if the proper apoptosis of myofibroblasts does not occur upon the cease of wound contraction [15-18]. Therefore, the fibroblast-to-myofibroblast differentiation needs to be appropriately balanced for minimum scar formation during the wound healing. It is well established that transforming growth factor-β (TGF-β) signaling could induce fibroblast-to-myofibroblast differentiation [19, 20]. However, it is unknown whether the cell-growing substrate can induce this fibroblast-to-myofibroblast differentiation independent of TGF-β signaling. A very recent result that rigid cell culture surface could promote the fibroblast-to-myofibroblast differentiation suggests a possible correlation between fibroblast-to-myofibroblast differentiation and their substrate [21]. Considering that nanofiber organization could modulate cellular morphology and migration, we therefore hypothesize that the fiber alignment may also affect fibroblast-to-myofibroblast differentiation and integrins may be involved as well.

To address this hypothesis together with the attempt to mechanistically understand fiber alignment-induced cell migration, normal human dermal fibroblasts (NHDFs) were seeded on collagen-containing PCL nanofibrous matrices with either isotropic nanofiber arrangement (*i.e.*, randomly collected nanofibers with no alignment, abbreviated as "*Iso*") or anisotropic nanofiber arrangement (*i.e.*, collected nanofibers with alignment, abbreviated as "*Aniso*"). The elongated cell morphology and accelerated migration of NHDFs along the fiber orientation were observed in the anisotropic fiber group. Both immunostaining and immunoprecipitation demonstrated the enhanced activation of integrin β1 by anisotropic collagen-containing PCL nanofibers. Treatment of NHDFs with integrin β1 neutralizing antibody clearly blocked the fiber-induced migration. Elevated expression of α-SMA was detected in NHDFs cultured on anisotropic matrices by real-time PCR and immunofluorescent staining, demonstrating that fiber alignment indeed induces fibroblast-to-myofibroblast differentiation. Blocking the cellular activity of integrin β1 also diminished this fibroblast-to-myofibroblast differentiation. Clearly, integrin β1 signaling played a crucial role in regulating the response of NHDFs to the spatial organization of collagen-containing nanofibers. This finding would provide a mechanistic guidance for the fabrication of functional skin grafts using electrospun nanofibers.

2. Materials and Methods

2.1. Materials

1,1,1,3,3,3-hexafluoro-2-propanol (HFIP) was obtained from Oakwood products Inc (West Columbia, SC). Poly (epsilon-caprolactone) (PCL, Mw=80,000) was purchased from Sigma-Aldrich (St. Louis, MO) and type I collagen (Coll) was obtained from Elastin Products Inc. (Owensville, MO). Fetal bovine serum (FBS) was purchased from American Type Culture Collection (ATCC, Manassas, VA). All other reagents and solutions were obtained from Invitrogen (Carlsbad, CA) except as indicated.

2.2. Nanofibrous matrix preparation

Nanofibrous matrices of PCL and Collagen at a weight ratio of 3:1 were fabricated using electrospinning as previously described [11]. Briefly, 8% (w/v) solution of 3:1 PCL/Coll was prepared by dissolving PCL and collagen in HFIP. Then, the solution was loaded into a 3-mL syringe with a 20-gauge stainless steel blunt-tip needle and electrospun at 15 kV using a custom electrospinning device. The polymer solution was dispensed using a syringe pump (Kdscientific, Holliston, MA) at 10 μL/min. Nanofibrous matrices with two types of fiber spatial organizations, *isotropic* and *anisotropic*, were prepared. To fabricate isotropic nanofibrous matrix, PCL/Coll nanofibers were collected on a grounded stationary aluminum plate surface, while the anisotropic PCL/Coll nanofibrous matrices were obtained by collecting the nanofibers onto a customized rotating mandrel (10 cm in diameter). Nanofibrous matrices collected on glass cover slips under sterile conditions were used for the studies unless indicated.

To characterize the electrospun nanofiber using a scanning electron microscope (SEM), fibers were collected on Si wafer and sputter-coated with gold. The coated fibers were examined with a LEO 982 FEG SEM. To determine the diameter of nanofibers, images of five randomly selected areas were captured and analyzed by NIS-elements BR 3.10 analysis software from Nikon. Tensile properties of the electrospun nanofibrous matrices were measured with a Rheometrics Solid Analyzer (RSA III; Rheometric Scientific Inc., Piscataway, NJ) at an extension rate of 0.05 mm/sec. All the samples were tested at 15 mm gauge length. Data were analyzed using TA Orchestrator (New Castle, DE).

The orientation of electrospun nanofibers was determined by using the ImageJ program (NIH) along with the Oval Profile Plot plugin [22]. Briefly, representative SEM images of the electrospun fibers were cropped into a square covering as much of the image as possible (the images used were 905 × 905 pixels in size). These cropped images were then processed with a fast Fourier transform (FFT) and then a circular selection of the image was made maximizing the amount selected (edges of the circle were tangent with the edges of the image). This selection then underwent a radial summation using the Oval Profile Plot plugin with 360 points such that the degree interval was 1°. The raw data were normalized to 0 and data from all sets were rescaled to an arbitrary range between 0 and 0.3. The final results were presented by plotting this arbitrary scale versus degrees, where the height of peaks represents a greater degree of alignment at a given angle.

2.3. Cell seeding and culture onto nanofibrous matrix

Normal primary human skin fibroblasts from newborn foreskin (R2F) were a gift from Dr. James G. Rheinwald of the Harvard NIH Skin Disease Research Center. The cells were grown in monolayer culture in the Dulbecco's modified Eagle medium (low glucose) supplemented with 10% fetal bovine serum and 1% penicillin and streptomycin (Sigma) at 37°C in a humidified 5% CO_2 atmosphere. Cells were routinely subcultured and used at passages 5-7.

The fibroblasts were seeded on the nanofibrous matrices at a density of 5×10^3 cells/cm^2 and allowed to attach for 60 min before fully supplemented media was added. The cells were cultured on the isotropic or anisotropic nanofibrous matrices for up to 7 days. The effects of nanofiber spatial organization on cell behaviors were determined throughout the 1-week culture period.

2.4. Immunofluorescence staining

Immunofluorescence staining of cells was performed as described previously [23]. Briefly, cultured cells were fixed in 4% paraformaldehyde for 20 minutes. Then, they were permeabilized with 0.2% Triton X-100 in PBS. Afterwards, cells were incubated with the following reagents, respectively: phalloidin-TRITC (Sigma, P1951, 1:500), anti-integrin β1 antibody against the active conformation of the β1 integrin (Millipore, clone HUTS-4, 1:300), anti-vinculin-FITC (Sigma, F7053, 1:200) and anti-paxillin (Millipore, clone 5H11, 1:200). For those primary antibodies without fluorescent labels, the cells were further incubated with goat anti-mouse IgG-FITC conjugate secondary antibody (Caltag, PAB4971, 1:400). Cell nuclei were stained with DAPI (Sigma, 1:1000). The staining was examined under a Nikon Eclipse 80i epifluorescent microscope. Fluorescence intensity of stained cells was quantified by using a multi-mode microplate reader (Synergy™ HT, BioTek Instruments, Inc., Winooski, VT).

2.5. Cell proliferation

Cell proliferation on nanofibrous matrices was determined by CyQUANT® Cell Proliferation Assay Kit (Molecular Probes, Inc., Eugene, OR) following the protocol suggested by the manufacturer. Briefly, A standard curve over cell number was first created ($y=10.94x+28.73$, $R^2=0.994$). Samples were then harvested on day 1, 3 and 7 (n=4 per group for each time point). After removal of media and washing with PBS, the samples were frozen and stored at −70°C. After collecting all the time-point samples, the samples were thawed at room temperature and then 200 μL of CyQUANT® GR dye/cell-lysis buffer was added to each sample and incubated for 2-5 minutes in the dark at room temperature. The fluorescence of cell lysates was measured using the multi-mode BioTek microplate reader at ~480 nm excitation and ~520 nm emission. Cell numbers were calculated based on the

standard curve. In addition, MTT assay for metabolic activity was also performed to confirm the DNA assay result [24].

2.6. Reverse transcription (RT)-PCR and real-time PCR (Q-PCR) analysis

Total RNA of the cultured cells was isolated using the Trizol reagent and subjected to reverse transcription for the first strand cDNA synthesis with superscript III reverse transcriptase following the manufacturer's protocol. RT-PCR was performed using the Eppendorf Mastercycler® (Hauppauge, NY). Q-PCR was performed with the Stratagene Mx3000P system (Agilent Technologies, La Jolla, CA) and analyzed as previously described [25]. Housekeeping genes, GAPDH and β-actin (data not shown), were used to normalize the target RNA. Primers for Q-PCR in this study were shown in Table 1.

2.7. Immunoprecipitation

Cells were lysed in radioimmunoprecipitation assay buffer (50 mM Tris, pH7.4, 150 mM NaCl, 1 mM EDTA, 1% NP-40, 0.25% deoxycholate) containing protease and phosphatase inhibitor cocktails. Protein concentrations were determined using bicinchroninic acid reagents (Pierce). For immunoprecipitation, equal amounts of proteins were precleared with protein G agarose and then incubated with anti-integrin β1 antibody (HUTS-4) and protein G agarose overnight. Immunoprecipitates were washed and analyzed by non-reducing SDS-PAGE and western blotting.

2.8. Western blotting

Cellular protein lysates were extracted from homogenized specimens in 150 mM NaCl, 10 mM Tris (pH 7.2), 0.1% SDS, 1% Triton X-100, 1% deoxycholate, and 5 mM EDTA. The protein lysates were denatured in Laemmli buffer at 90°C for 15 minutes. Then they were loaded on a 10% SDS-PAGE gel, and subjected to electrophoresis under reducing conditions. Proteins were transferred onto a polyvinylidene difluoride membrane (Kodak, Rochester, NY) following the standard protocol. After blocking in 5% fat-free milk in PBS for 1 hour, the membrane was incubated overnight with primary antibody at 4°C. Antibodies used in Western blotting are as follows: Anti-FAK (Millipore, 05-537, 1:5000), Anti-FAK-Tyr397 (BD biosciences, 611806, 1:1000), Anti-integrin β1 (Millipore, MAB2079Z, 1:1000; MAB1987, 1:1000), Anti-GAPDH (Millipore, MAB374, 1:5000), Anti-β-actin (Sigma, A5316, 1:5000). The membrane was washed, and then incubated with horseradish peroxidase-conjugated secondary antibody (Invitrogen, 1:4,000) at room temperature. Detection was performed using enhanced chemiluminescence (ECL, GE Health, UK).

2.9. Wound healing assay

In vitro CytoSelect™ 24-Well Wound Healing Assay Kit purchased from Cell Biolabs Inc. (San Diego, CA) was used to evaluate the migratory behavior of fibroblasts. Briefly, 5×10^4 fibroblasts suspended in culture media were seeded onto the surfaces of nanofibrous matrices with inserts in the middle. After 24 hours, the insert was removed to generate a consistent 0.9-mm wound gap in the middle. Cells were allowed to migrate into the wound gap on either isotropic or anisotropic nanofibrous matrices for 24 and 48 hours. After fixation, cells were stained with methylene blue and images of the wound gap were taken to analyze the migration distance of fibroblasts. At least 10 representative points along the "wound" of each sample were used for evaluating the migration rate from 4 separate samples (n=4) for each time point.

3.0. Statistical Analysis

Each experiment was repeated at least 3 times on different days and data were expressed as the mean ±SD. All the cytotoxicity and cell attachment measurements were collected in

triplicate for each group. An unpaired student t-test was used to evaluate the significance among experimental groups. A value of $p<0.05$ was considered statistically significant.

3. Results

3.1. Characterization of PCL/collagen nanofibrous matrices

Using the established electrospinning condition as described in Materials and Methods, PCL/Coll nanofibers collected on a rotating mandrel or on a stationary surface had distinct spatial arrangements (anisotropic *versus* isotropic) (Figure 1A and B). A majority of the fibers (~90%) collected on the rotating mandrel aligned in the same direction as the rotation. To better analyze the fiber alignment, FFT analysis was performed on the SEM images of randomly selected area (n=5) to characterize the anisotropy and assign a numerical value to fiber orientation. The narrow peak of the normalized intensity values in anisotropic matrices (Figure 1C) indicated that PCL/Coll nanofibers aligned along a single axis (Fig. 1B). In contrast, the lack of significant peak for the fibers collected on a stationary surface demonstrated no preferred fiber orientation in the isotropic matrices (Fig. 1C). The average fiber diameter for both matrices was comparable (*Aniso*, 313.33±69.52 nm *vs. Iso*, 331.11±112.05 nm) (Figure 1D). Close examination of the nanofiber surface with SEM revealed a relatively smooth surface for both isotropic and anisotropic nanofibers (data not shown). Compared to isotropic matrices, the freestanding anisotropic matrices showed higher ultimate stress (*Aniso*, 1.07 ± 0.19 MPa *vs. Iso*, 0.60 ± 0.09 MPa) and Young's modulus (*Aniso*, 8.98±3.72 MPa *vs. Iso*, 2.83 ± 0.60 MPa) in the alignment.

3.2. Cellular morphology and proliferation

To determine the cell morphology on various nanofibrous matrices, NHDFs cultured on either isotropic or anisotropic nanofibrous matrices collected on glass cover slips, were immunostained for focal adhesion proteins, vinculin and paxillin. The actin cytoskeleton was visualized with TRITC-labeled phalloidin. After 3-day culture, F-actin staining showed that NHDFs appeared to be polygonal on the isotropic matrices without preferred orientation despite certain orientation of actin filaments within individual cells (Figure 2A, arrows). Interestingly, the cells on anisotropic matrices became elongated with a majority of the actin filaments oriented in the same direction as aligned PCL/collagen nanofibers (Figure 2A). Close examination of the organization of actin filaments showed that they remained as compact bundles instead of individual actin filaments like those on isotropic matrices. The staining for focal adhesion associated proteins indicated that nanofiber orientation affected the spatial distribution of focal adhesion plaques on cell membranes. On anisotropic matrices, long segments of vinculin were stained along the nanofiber alignment, but on the isotropic matrices no preferred orientation was observed (Figure 2B, arrows). On both matrices, vinculin clusters mainly located on the circumferential region of cell membranes directly contacted with nanofibers. Similarly, elongated paxillin was observed along the fiber alignment on the anisotropic matrices and randomly distributed paxillin was seen on the isotropic matrices (Figure 2C, arrows). They evenly distributed across the cell membrane on both matrices.

The proliferation of NHDFs on both PCL/Coll nanofiber matrices was determined by DNA assay and MTT assay for up to 7 days. No statistical difference was identified between the two groups on day 1, 3 and 7 (Figure 3 and Supplemental Figure). A time-dependent increase of cell number on both nanofibrous matrices demonstrated the biocompatibility and supportiveness of PCL/Coll nanofibers for fibroblast proliferation.

3.3. Activation of integrin β1 in fibroblasts by anisotropic nanofibrous matrices

Integrins of the β1 subfamily are the major ECM receptors present in fibroblasts. Integrin β1 is synthesized and partially glycosylated on rough endoplasmic reticulum (ER). This precursor is further processed in Golgi apparatus by glycosyltransferases to generate fully glycosylated mature form prior to transport to the plasma membrane. In fibroblasts cultured on the plastic surface, the ECM-cell interaction activates integrin β1 and induces focal adhesion formation. However, little is known about the modulation of integrin β1 activity by nanofibrous matrices. To examine the activation of integrin β1 in NHDFs by various nanofibrous matrices, immunofluorescent staining was performed 3 hours after the cells were seeded to detect the active conformation of integrin β1 using the monoclonal antibody HUTS-4. As shown in Figure 4A (arrows), a significant amount of active integrin β1 was observed on the edge of NHDFs cultured on the anisotropic matrices compared to those on the isotropic matrices. Although the cells did not spread completely, which resulted in the enriched strong signals of integrin β1 in cell bodies, the activation of integrin β1 at the newly formed cellular edge was detected. The active integrin β1 mainly located along the anisotropic nanofibers with a similar anisotropic pattern. Furthermore, quantitative analysis of active integrin β1 by measuring the fluorescence intensity of labeled cells confirmed that active integrin β1 level was significantly higher on the anisotropic matrices than that on the isotropic ones ($p<0.01$) (Figure 4B). Similarly, immunoprecipitation with the antibody HUTS-4 pulled down the 130 kD mature, active form of integrin β1 (Figure 4D), which was increased by 58% in the cells on the anisotropic matrices compared to those on the isotropic ones (Figure 4E). The under glycosylated immature integrin β1 (105 kD) was not detected in the immunoprecipitates. Both semi-quantitative analysis of integrin β1 gene expression by Q-PCR and total integrin β1 protein level by western blot revealed that there was no significant difference between isotropic and anisotropic groups (Figure 4C, 4D and 4E). These results suggest that the alignment of nanofibers may induce integrin signaling by activating integrin β1 without modulating the total integrin β1 level.

3.4. Phosphorylation of FAK in fibroblasts enhanced by anisotropic nanofibrous matrices

The differential activation of integrin β1 by nanofibrous matrices suggests the possibility that various nanofiber spatial organizations may trigger outside-in signaling in NHDFs through integrin β1. It is known that FAK, one of the most critical integrin signaling molecules, is activated through autophosphorylation at tyrosine 397 upon integrin β1 activation. To confirm this, the FAK phosphorylation level in cultured NHDFs was determined by western blotting. It was found that FAK phosphorylation at Tyr-397 was significantly increased in the NHDFs cultured on anisotropic matrices despite a comparable expression of total FAK on both isotropic and anisotropic matrices (Figure 5). Thus, our results suggest that fiber organization in nanofibrous matrices may regulate the integrin-FAK signaling pathway in NHDFs.

3.5. Role of integrin β1 in fibroblast migration on various nanofibrous matrices

In order to evaluate the effects of various fiber organizations (*i.e.*, isotropic *vs.* anisotropic) on NHDF migration, an *in vitro* wound-healing assay was performed by culturing cells on various matrices with “wound gaps” created by an insert (Figure 6A). The culture stained with methylene blue after 24 and 48 hrs revealed that the migration of NHDFs was significantly regulated by the underlying nanofiber organization. On the isotropic matrices, NHDFs barely migrated into the “wound gap” after 24 hr culture and only provided a moderate wound coverage (about 50%) after 48 hr (Figure 6A and B). In contrast, on the anisotropic matrices, NHDF migration into the wound area was greatly enhanced along the fiber alignment and the “wound gap” was completely closed by 48 hrs (Figure 6A and B). In order to determine the role of integrin β1 in fibroblast motility on these collagen-containing nanofibers, we also did the wound-healing assay by blocking the NHDF integrin β1 activity

with integrin β1 neutralizing antibody. Apparently, the antibody significantly inhibited NHDF migration on the anisotropic fibers. Even after 48 hr, the "wound gap" remained unclosed (Figure 6A) and only approximately 60% wound closure was achieved (Figure 6B). These results suggested that the promotion of fibroblast migration on anisotropic collagen-containing nanofibrous matrices is mediated by β1 integrins.

3.6. Promotion of myofibroblastic differentiation by anisotropic nanofibers

Differentiation of fibroblasts into myofibroblasts and the consequent wound contraction are important processes in wound healing. The expression of alpha-smooth muscle actin (α-SMA) is considered as a specific marker for myofibroblast differentiation. To address whether the organization of PCL/Coll nanofibers regulated the fibroblast-to-myofibroblast differentiation, NHDFs cultured on isotropic and anisotropic nanofibrous matrices were examined for their gene expression of α-SMA by using both RT-PCR and Q-PCR. A significantly higher expression of α-SMA gene (ACTA2, NM_001613.2) was measured on the NHDFs cultured for 48 hrs on the anisotropic matrices in comparison to those cultured on the isotropic matrices (Figure 7A and B). Consistent with the gene expression results, immunofluorescent staining for α-SMA further confirmed that nanofiber alignment indeed stimulated the fibroblast-to-myofibroblast differentiation of NHDFs, evidenced by a significant increase of α-SMA positive cells in the cultured NHDFs (Figure 7C and D). To examine whether integrin β1 was involved in myofibroblastic differentiation, integrin β1 neutralizing antibody was added to the culture while culturing NHDFs on various nanofibrous matrices. It was found that with the integrin β1 neutralizing antibody, the percentage of α-SMA positive cells was significantly reduced on the anisotropic matrices (Figure 7C and D), suggesting that integrin β1 was involved in the regulation of fibroblast-to-myofibroblast differentiation by anisotropic nanofibers.

Discussion

The utilization of biomimetic nanofibers for wound healing and tissue-engineered skin grafts has shown multifold advantages in promoting tissue formation and facilitating wound closure, while insightful understanding of nanofiber-regulated phenotype of fibroblasts becomes an emerging demand. In this study, we have shown that anisotropic PCL/collagen nanofibers could activate the integrin β1 in the membrane of NHDFs and increase the phosphorylation of FAK, a critical downstream kinase of integrin signaling. By using a wound-healing model and antibody blockade treatment, we have demonstrated that the accelerated fibroblast migration on anisotropic PCL/collagen nanofibers is mediated by integrin β1. More importantly, we have found that these anisotropic nanofibers significantly promote the fibroblast-to-myofibroblast differentiation, but the blockade of integrin β1 activity abolishes this differentiation. These findings suggest that integrin β1-FAK signaling is an important mechanism to regulate the migration and differentiation of fibroblasts on collagen-containing nanofibrous matrices.

Increasing evidence has shown that the cellular microenvironment greatly regulates cellular responses such as adhesion, spreading, proliferation and migration. This regulation is closely related to the substrate rigidity and topography via mechanotransduction in addition to chemical stimulation [21, 26-28]. Several studies have investigated the effect of electrospun nanofiber organization on the morphology and migration of fibroblasts [9-12]. Consistent with those observations, we also found that NHDFs became elongated on anisotropic nanofibrous matrices (Figure 2). Although higher Young's modulus was indeed measured on freestanding anisotropic PCL/Coll nanofibrous matrices along the alignment compared to isotropic ones (*aniso*, 8.98±3.72 MPa *vs. iso*, 2.83 ± 0.60 MPa), this mechanical contribution could be neglected in this study due to the use of rigid glass cover slips as collection surfaces for both matrices and being used through the entire study. In addition, the

comparable average nanofiber diameters in both matrices (331nm *vs.* 313nm) also exclude the possible contribution of fiber diameter. Thus, this morphology variation mainly comes from the fiber organization, and is plausibly controlled by the formation and distribution of focal adhesion plaques between nanofibers and cell membrane. As shown in Figure 2, long segment staining of both paxillin and vinculin was observed along the aligned PCL/Coll nanofibers and located on the cell-nanofiber contact regions. The formation of focal adhesions is mediated by integrin receptors on the cell surface. The engagement of integrins to ECM ligands leads to integrin activation (outside-in signaling) and activated integrins in turn recruit focal adhesion proteins such as paxillin, vinculin, talin, and kindlin to the cell-matrix adhesion site. The binding of talin and kindlin to the integrin β cytoplasmic tail can further enhance integrin activation (inside-out signaling). It is unclear, however, whether these signaling events are regulated by anisotropy of cell adhesive microenvironment. Our new data showed that anisotropic PCL/Coll nanofibers could selectively enhance integrin β1 activation (Figure 4B and 4D) and the activated integrin β1 mainly located in the front edge of fibroblasts along both the polarized F-actin filaments inside the cell and the outside nanofibers (Figure 4A). We speculate that the polarized distribution of F-actin filaments, which are connected to integrins through talin and kindlin, may be involved in the amplification of integrin activation. This nanofiber-induced activation of integrin β1 may be further transmitted to its downstream effectors. FAK, a cytoplasmic protein tyrosine kinase, is an important mediator of integrin signaling and co-localizes with integrin β1 at focal adhesions. The phosphorylation of FAK primarily occurs at the Y397 site upon integrin β1 activation [29, 30]. In this study, FAK phosphorylation at Y397 in NHDFs was significantly elevated on anisotropic nanofibrous matrices despite a constant expression of FAK on both matrices. Phosphorylated FAK may regulate multiple cellular functions such as cell adhesion and migration by further activating downstream signaling molecules such as Src and PI3K [31]. Cell migration is a complex and highly coordinated process, greatly depending upon dynamic integrin-matrix interactions [32-34]. Previous study illustrated the establishment of integrin-mediated focal adhesions at the front protrusions and the disassembly of these adhesion complexes at the tail region of migrating fibroblasts [35]. In our study, the abrogation of facilitated cell migration by integrin β1 neutralizing antibody (Figure 6) implies the crucial role of integrin β1 signaling in fibroblast migration on anisotropic PCL/Coll nanofibers and the increased phosphorylation of FAK at Y397 may induce the rapid turnover of focal adhesions at the trailing edge to promote cell motility [36-38].

Fibroblast-to-myofibroblast differentiation, important to the reconstruction of connective tissue during wound healing, is promoted by TGF-β1 and mechanical stress [39-42]. In TGF-β1-regulated myofibroblastic differentiation, FAK expression is critical to both ERK and p38 activation that are required for TGF-β1-induced α-SMA expression [43]. Spatial organization of FAK is well connected to the intracellular distribution of α-SMA stress fibers and greatly correlated with the mature of myofibroblastic differentiation [44]. Whereas in the present study no exogenous TGF-β1 was supplemented to the culture, to our surprise, higher expression of α-SMA gene (ACTA2) was still detected on the NHDFs cultured on anisotropic PCL/Coll nanofibrous matrices (Figure 7A and B). Fluorescent staining for α-SMA further confirmed this observation (Figure 7C and D). Interestingly, the blockade of integrin β1 activity with neutralizing antibody almost completely abolished the α-SMA promotion effect by anisotropic PCL/Coll nanofibers (Figure 7C and D). It has been noted that anisotropic PCL/Coll nanofibers could activate integrin β1 and promote the phosphorylation of FAK (Figure 4 and 5). The phosphorylation of FAK may lead to the activation of ERK and p38 mediators for α-SMA [43]. Further investigation on the ERK and p38 activity on anisotropic PCL/Coll nanofibers is necessary to confirm the regulatory involvement of this pathway. Additionally, it has been reported that fibroblast-to-myofibroblast transition in collagen gel could be promoted by interstitial fluid flow, as a

result of the aligned force imposed on the fibroblasts by fluid flow [45]. However, in this study no medium flow was offered to the culture, which excluded this possible contribution. Necessary to mention, although in this study the potential contribution of mechanical differences between isotropic and anisotropic matrices to the cellular responses was neglected considering that the same highly rigid glass cover slips were used for the collected PCL/Coll nanofibers, studies on the mechanical stimuli are surely required for creating tissue-engineered skin grafts [46].

Conclusions

The present study demonstrated the dual functions of integrin β1 in mediating both fibroblast migration and fibroblast-to-myofibroblast differentiation on anisotropic collagen-containing nanofibers. NHDFs cultured on anisotropic PCL/collagen nanofibers showed elongated cell morphology, distinct distribution of focal adhesions, accelerated cell migration and promoted fibroblast-to-myofibroblast differentiation. The activation of the integrin β1-FAK signaling pathway by anisotropic nanofibers and the elimination of nanofiber-induced cellular responses by blocking integrin β1 activity both prove the important role of integrin β1 signaling in fibroblast migration and differentiation regulated by various spatial arrangements of collagen-containing nanofibers.

Supplementary Material

Refer to Web version on PubMed Central for supplementary material.

Acknowledgments

This investigation was sponsored by Grant Number 1R21 AR056416 from NIAMS. Xiaoling Fu is also supported by Innovation & Entrepreneurship Doctoral Fellowship from Stevens Institute of Technology.

References

[1]. MacNeil S. Progress and opportunities for tissue-engineered skin. Nature. 2007; 445:874–80. [PubMed: 17314974]

[2]. Ma Z, Kotaki M, Inai R, Ramakrishna S. Potential of nanofiber matrix as tissue-engineering scaffolds. Tissue Eng. 2005; 11:101–9. [PubMed: 15738665]

[3]. Kumbar SG, James R, Nukavarapu SP, Laurencin CT. Electrospun nanofiber scaffolds: engineering soft tissues. Biomed Mater. 2008; 3:034002. [PubMed: 18689924]

[4]. Venugopal J, Ramakrishna S. Biocompatible nanofiber matrices for the engineering of a dermal substitute for skin regeneration. Tissue Eng. 2005; 11:847–54. [PubMed: 15998224]

[5]. Yang X, Shah JD, Wang H. Nanofiber enabled layer-by-layer approach toward three-dimensional tissue formation. Tissue Eng Part A. 2009; 15:945–56. [PubMed: 18788981]

[6]. Miyata T, Taira T, Noishiki Y. Collagen engineering for biomaterial use. Clin Mater. 1992; 9:139–48. [PubMed: 10149963]

[7]. Powell HM, Supp DM, Boyce ST. Influence of electrospun collagen on wound contraction of engineered skin substitutes. Biomaterials. 2008; 29:834–43. [PubMed: 18054074]

[8]. Yang X, Ogbolu KR, Wang H. Multifunctional nanofibrous scaffold for tissue engineering. J Exp Nanosci. 2008; 3:329–345.

[9]. Dalby MJ, Riehle MO, Johnstone HJ, Affrossman S, Curtis AS. Polymer-demixed nanotopography: control of fibroblast spreading and proliferation. Tissue Eng. 2002; 8:1099–108. [PubMed: 12542955]

[10]. Venugopal JR, Zhang Y, Ramakrishna S. In vitro culture of human dermal fibroblasts on electrospun polycaprolactone collagen nanofibrous membrane. Artif Organs. 2006; 30:440–6. [PubMed: 16734595]

[11]. Zhang YZ, Venugopal J, Huang ZM, Lim CT, Ramakrishna S. Characterization of the surface biocompatibility of the electrospun PCL-collagen nanofibers using fibroblasts. Biomacromolecules. 2005; 6:2583–9. [PubMed: 16153095]

[12]. Xie J, Macewan MR, Ray WZ, Liu W, Siewe DY, Xia Y. Radially aligned, electrospun nanofibers as dural substitutes for wound closure and tissue regeneration applications. ACS Nano. 2010; 4:5027–36. [PubMed: 20695478]

[13]. Fu X, Wang H. Spatial arrangement of polycaprolatonec/collagen nanofibrous scaffolds regulates the wound-healing related behaviors of human adipose stromal cells. Tissue Eng Part A. Epub ahead of print.

[14]. Yang, X.; Wang, H. Electrospun functional nanofibrous scaffolds for tissue engineering. In: Eberli, D., editor. Tissue Engineering. InTech; Croatia: 2010. p. 159-176.

[15]. Martin P. Wound healing--aiming for perfect skin regeneration. Science. 1997; 276:75–81. [PubMed: 9082989]

[16]. Singer AJ, Clark RA. Cutaneous wound healing. N Engl J Med. 1999; 341:738–46. [PubMed: 10471461]

[17]. Darby IA, Hewitson TD. Fibroblast differentiation in wound healing and fibrosis. Int Rev Cytol. 2007; 257:143–79. [PubMed: 17280897]

[18]. Hinz B. Formation and function of the myofibroblast during tissue repair. J Invest Dermatol. 2007; 127:526–37. [PubMed: 17299435]

[19]. Desmouliere A, Geinoz A, Gabbiani F, Gabbiani G. Transforming growth factor-beta 1 induces alpha-smooth muscle actin expression in granulation tissue myofibroblasts and in quiescent and growing cultured fibroblasts. J Cell Biol. 1993; 122:103–11. [PubMed: 8314838]

[20]. Vi L, de Lasa C, DiGuglielmo GM, Dagnino L. Integrin-linked kinase is required for TGF-beta1 induction of dermal myofibroblast differentiation. J Invest Dermatol. 2011; 131:586–93. [PubMed: 21150927]

[21]. Li Z, Dranoff JA, Chan EP, Uemura M, Sevigny J, Wells RG. Transforming growth factor-beta and substrate stiffness regulate portal fibroblast activation in culture. Hepatology. 2007; 46:1246–56. [PubMed: 17625791]

[22]. Ayres C, Bowlin GL, Henderson SC, Taylor L, Shultz J, Alexander J, et al. Modulation of anisotropy in electrospun tissue-engineering scaffolds: Analysis of fiber alignment by the fast Fourier transform. Biomaterials. 2006; 27:5524–34. [PubMed: 16859744]

[23]. Eisenbarth E, Meyle J, Nachtigall W, Breme J. Influence of the surface structure of titanium materials on the adhesion of fibroblasts. Biomaterials. 1996; 17:1399–403. [PubMed: 8830966]

[24]. Hansen MB, Nielsen SE, Kurt B. Re-examination and further development of a precise and rapid dye method for measuring cell growth/cell kill. J Immunol Methods. 1989; 119(2):203–210. [PubMed: 2470825]

[25]. Yuan JS, Reed A, Chen F, Stewart CN Jr. Statistical analysis of real-time PCR data. BMC Bioinformatics. 2006; 7:85. [PubMed: 16504059]

[26]. Webster TJ, Ergun C, Doremus RH, Siegel RW, Bizios R. Enhanced osteoclast-like cell functions on nanophase ceramics. Biomaterials. 2001; 22:1327–33. [PubMed: 11336305]

[27]. Dalby MJ, Di Silvio L, Gurav N, Annaz B, Kayser MV, Bonfield W. Optimizing HAPEX topography influences osteoblast response. Tissue Eng. 2002; 8:453–67. [PubMed: 12167231]

[28]. Dalby MJ. Topographically induced direct cell mechanotransduction. Med Eng Phys. 2005; 27:730–42. [PubMed: 15921949]

[29]. Sieg DJ, Hauck CR, Schlaepfer DD. Required role of focal adhesion kinase (FAK) for integrin-stimulated cell migration. J Cell Sci. 1999; 112(Pt 16):2677–91. [PubMed: 10413676]

[30]. Schlaepfer DD, Mitra SK. Multiple connections link FAK to cell motility and invasion. Curr Opin Genet Dev. 2004; 14:92–101. [PubMed: 15108811]

[31]. Mitra SK, Schlaepfer DD. Integrin-regulated FAK-Src signaling in normal and cancer cells. Curr Opin Cell Biol. 2006; 18:516–23. [PubMed: 16919435]

[32]. Palecek SP, Loftus JC, Ginsberg MH, Lauffenburger DA, Horwitz AF. Integrin-ligand binding properties govern cell migration speed through cell-substratum adhesiveness. Nature. 1997; 385:537–40. [PubMed: 9020360]

[33]. Giancotti FG, Ruoslahti E. Integrin signaling. Science. 1999; 285:1028–32. [PubMed: 10446041]

[34]. Harburger DS, Calderwood DA. Integrin signalling at a glance. J Cell Sci. 2009; 122:159–63. [PubMed: 19118207]

[35]. Palecek SP, Schmidt CE, Lauffenburger DA, Horwitz AF. Integrin dynamics on the tail region of migrating fibroblasts. J Cell Sci. 1996; 109:941–52. [PubMed: 8743941]

[36]. Yamada KM, Miyamoto S. Integrin transmembrane signaling and cytoskeletal control. Curr Opin Cell Biol. 1995; 7:681–9. [PubMed: 8573343]

[37]. Takagi J, Petre BM, Walz T, Springer TA. Global conformational rearrangements in integrin extracellular domains in outside-in and inside-out signaling. Cell. 2002; 110:599–11. [PubMed: 12230977]

[38]. Hamadi A, Bouali M, Dontenwill M, Stoeckel H, Takeda K, Ronde P. Regulation of focal adhesion dynamics and disassembly by phosphorylation of FAK at tyrosine 397. J Cell Sci. 2005; 118:4415–4425. [PubMed: 16159962]

[39]. Desmouliere A, Geinoz A, Gabbiani F, Gabbiani G. Transforming growth factor-beta 1 induces alpha-smooth muscle actin expression in granulation tissue myofibroblasts and in quiescent and growing cultured fibroblasts. J Cell Biol. 1993; 122:103–11. [PubMed: 8314838]

[40]. Vaughan MB, Howard EW, Tomasek JJ. Transforming growth factor-beta1 promotes the morphological and functional differentiation of the myofibroblast. Exp Cell Res. 2000; 257:180–9. [PubMed: 10854066]

[41]. Chan MW, Chaudary F, Lee W, Copeland JW, McCulloch CA. Force-induced myofibroblast differentiation through collagen receptors is dependent on mammalian diaphanous (mDia). J Biol Chem. 2010; 285:9273–81. [PubMed: 20071339]

[42]. Hinz B, Mastrangelo D, Iselin CE, Chaponnier C, Gabbiani G. Mechanical tension controls granulation tissue contractile activity and myofibroblast differentiation. Am J Pathol. 2001; 159:1009–20. [PubMed: 11549593]

[43]. Ding Q, Gladson CL, Wu H, Hayasaka H, Olman MA. Focal adhesion kinase (FAK)-related non-kinase inhibits myofibroblast differentiation through differential MAPK activation in a FAK-dependent manner. J Biol Chem. 2008; 283:26839–49. [PubMed: 18669633]

[44]. Dugina V, Fontao L, Chaponnier C, Vasiliev J, Gabbiani G. Focal adhesion features during myofibroblastic differentiation are controlled by intracellular and extracellular factors. J Cell Sci. 2001; 114:3285–96. [PubMed: 11591817]

[45]. Ng CP, Hinz B, Swartz MA. Interstitial fluid flow induces myofibroblast differentiation and collagen alignment in vitro. J Cell Sci. 2005; 118:4731–9. [PubMed: 16188933]

[46]. Lee CH, Shin HJ, Cho IH, Kang YM, Kim IA, Park KD, Shin JW. Nanofiber alignment and direction of mechanical strain affect the ECM production of human ACL fibroblast. Biomaterials. 2005; 26:1261–70. [PubMed: 15475056]

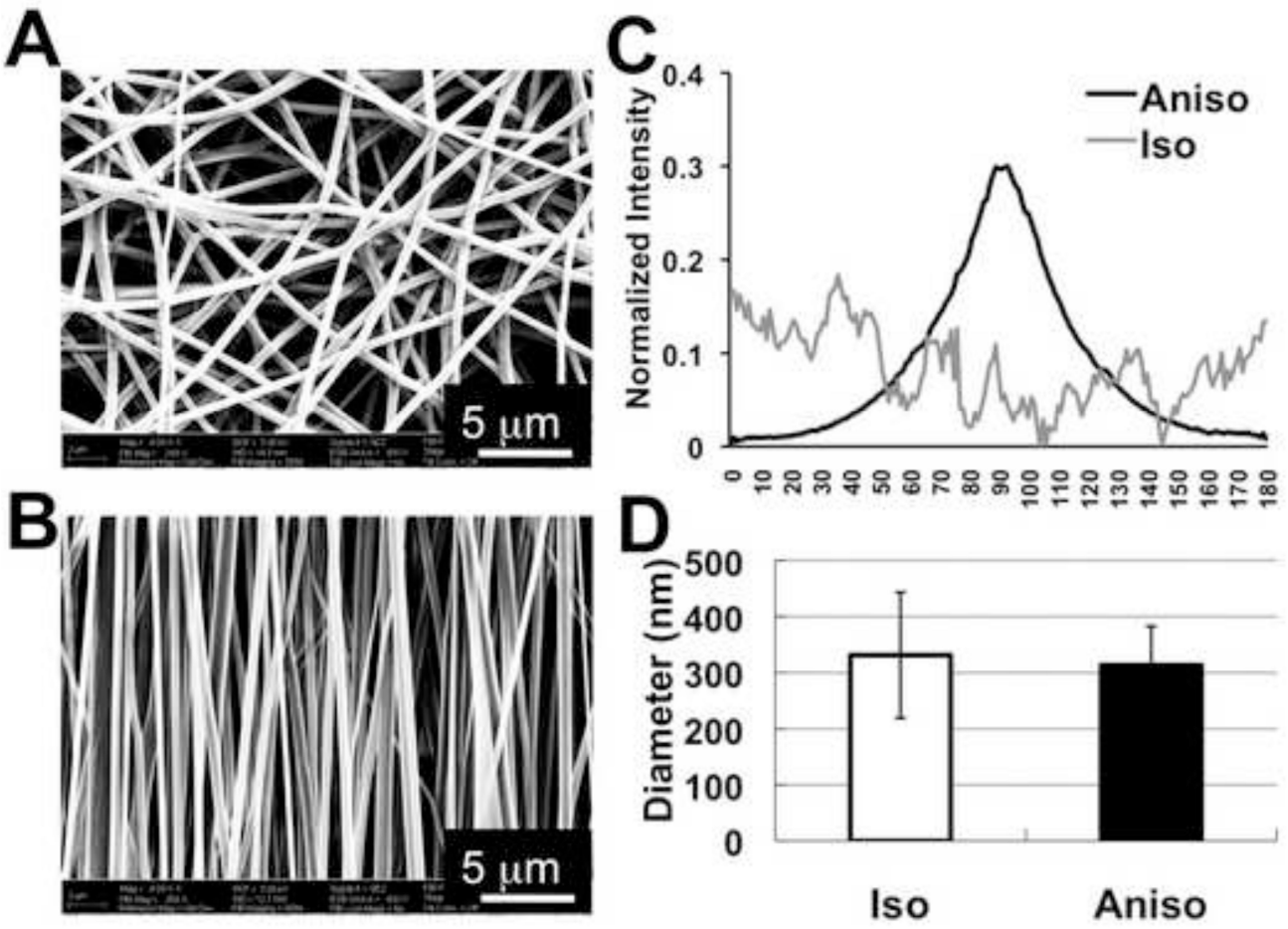

Figure 1.

Characterization of *isotropic* and *anisotropic* electrospun PCL/Coll nanofibrous matrices. SEM image of nanofibrous matrices with two types of fiber spatial organizations: *isotropic* (A) and *anisotropic* (B). (C) Normalized intensity plots against the angle of acquisition for *isotropic* and *anisotropic* nanofibrous matrices. (D) The measured average fiber diameter based on SEM images. Scale bar: 5μm.

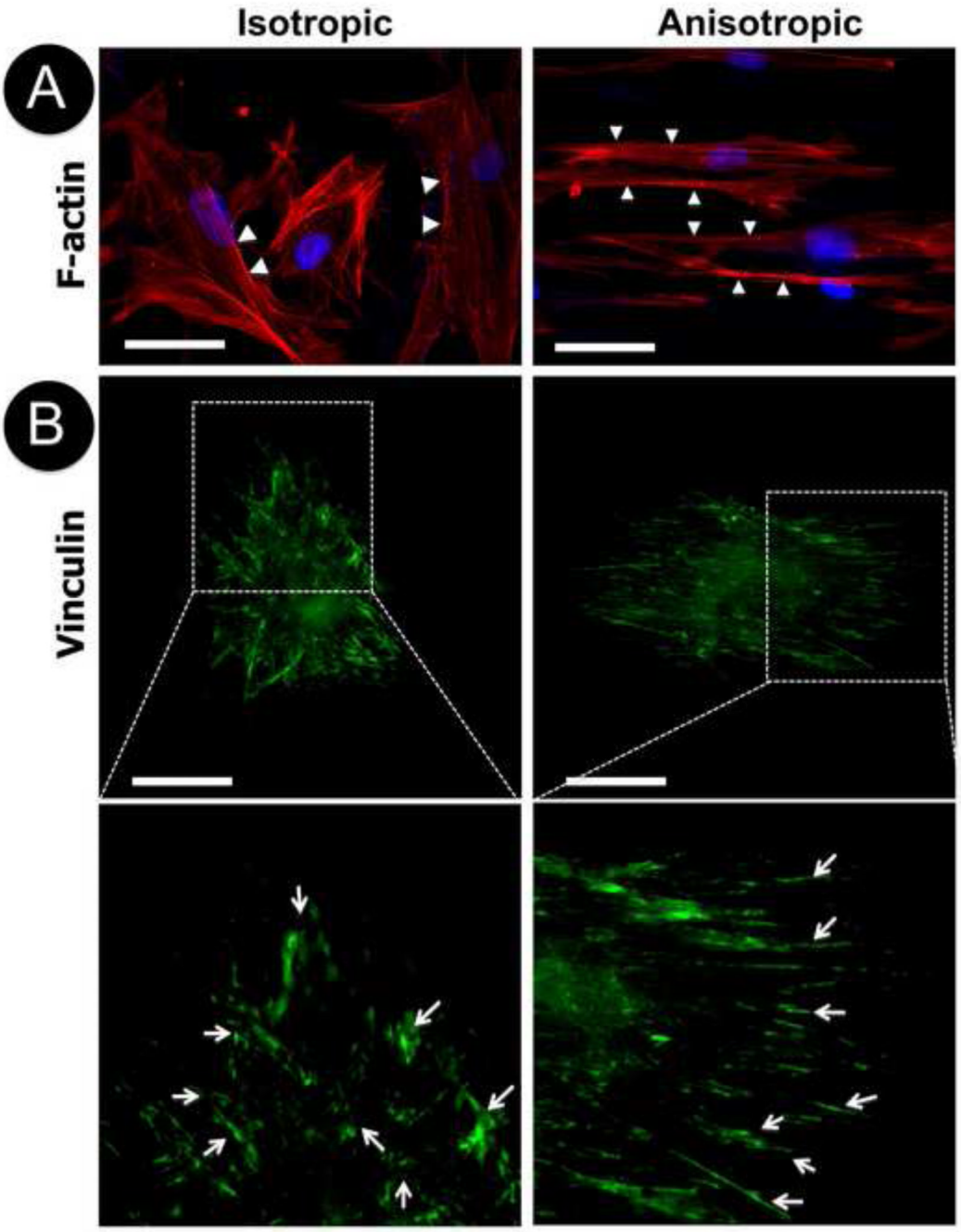

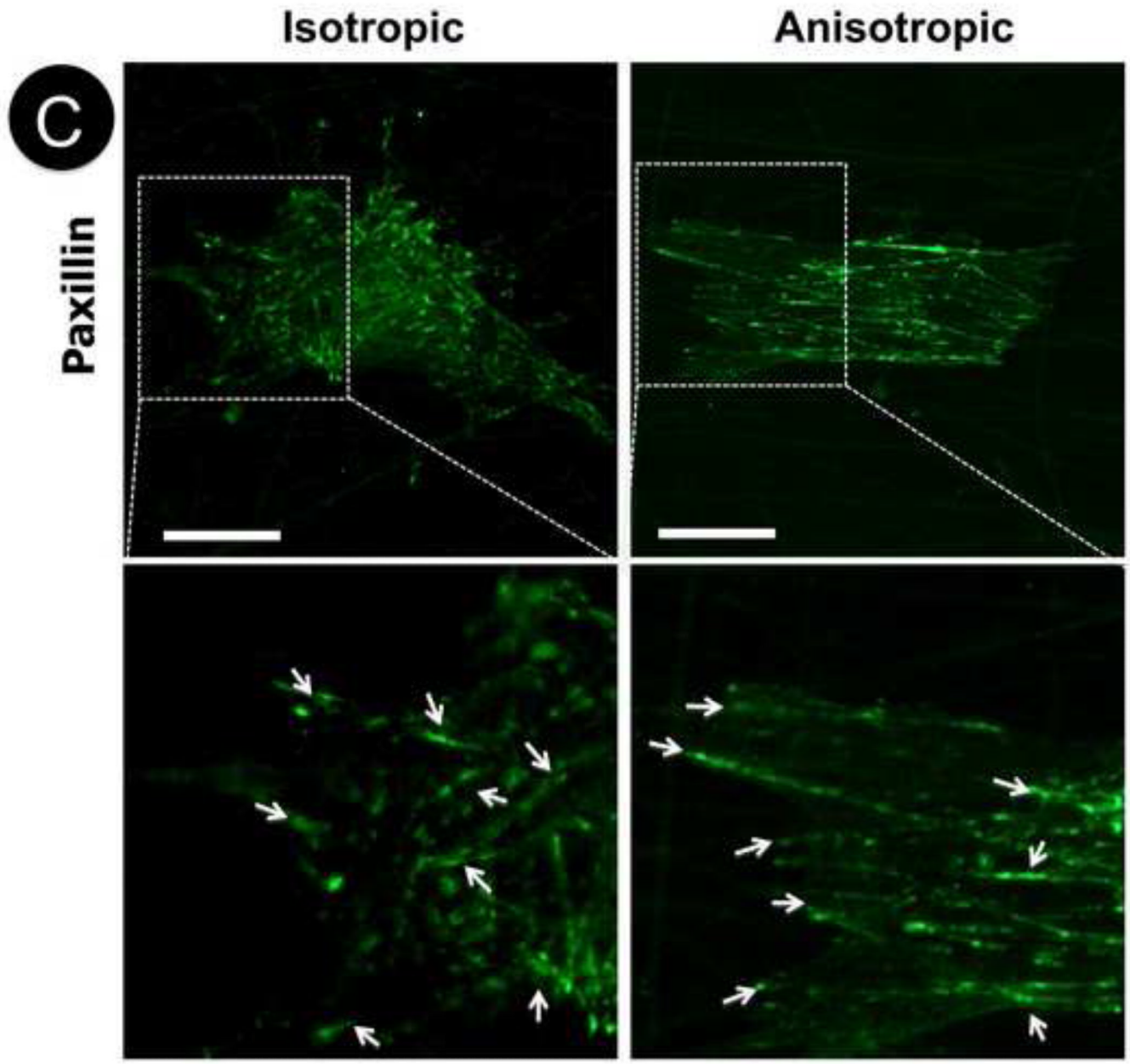

Figure 2.
Cellular morphology of human dermal fibroblasts on *isotropic* and *anisotropic* PCL/Coll nanofibrous matrices. Immunofluorescent staining of intracellular cytoskeleton protein of F-actin (red/orange) and nuclei with DAPI (purple/blue) (A), and focal adhesion proteins of vinculin (green) (B) and paxillin (green) (C). White arrows indicate spatial distribution of F-actin, vinculin or paxillin. Scale bar: 50μm.

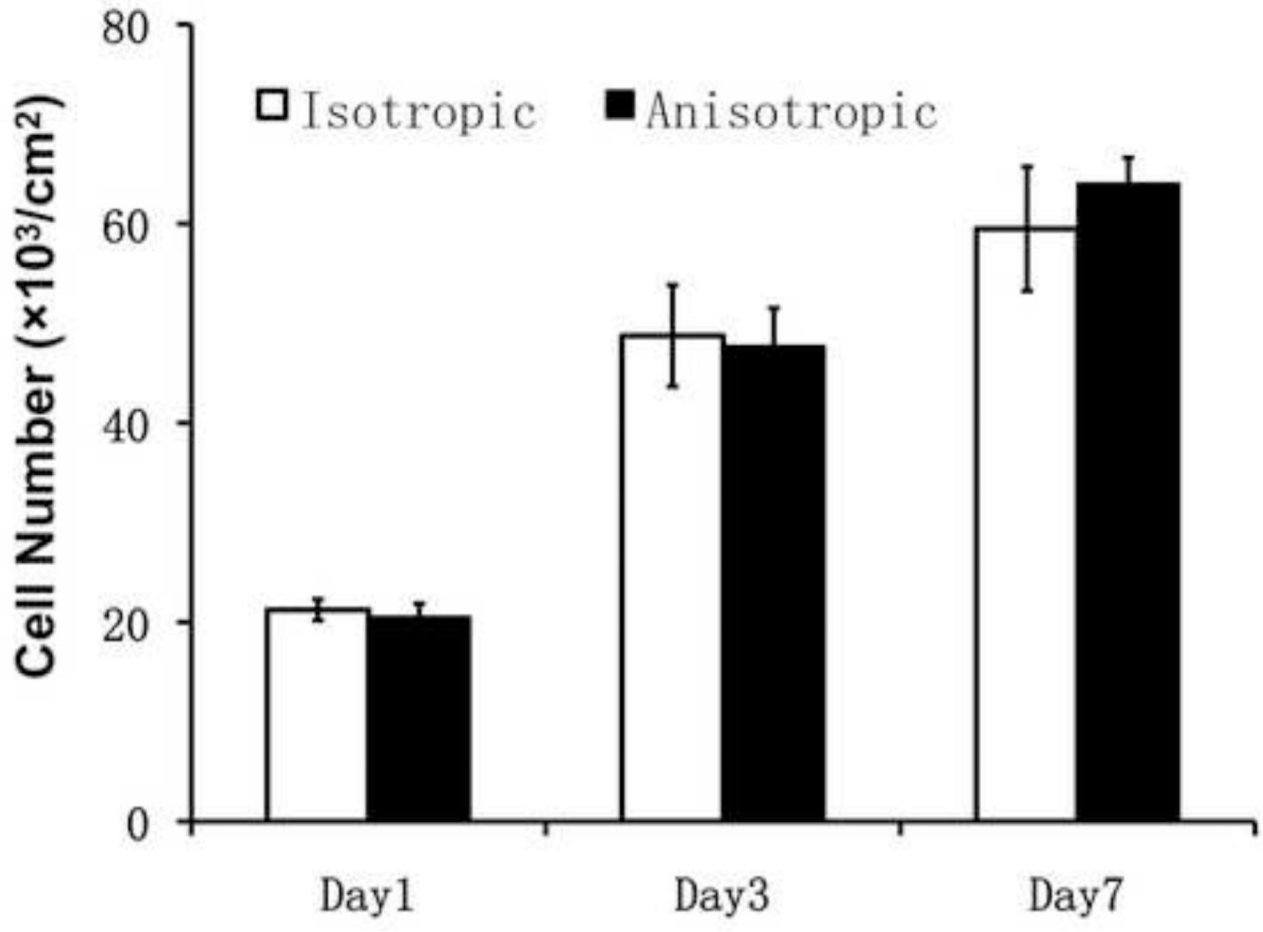

Figure 3.
Cell proliferation on either *isotropic* or *anisotropic* PCL/Coll nanofibrous matrices for up to 7 days determined by DNA assay (n=4).

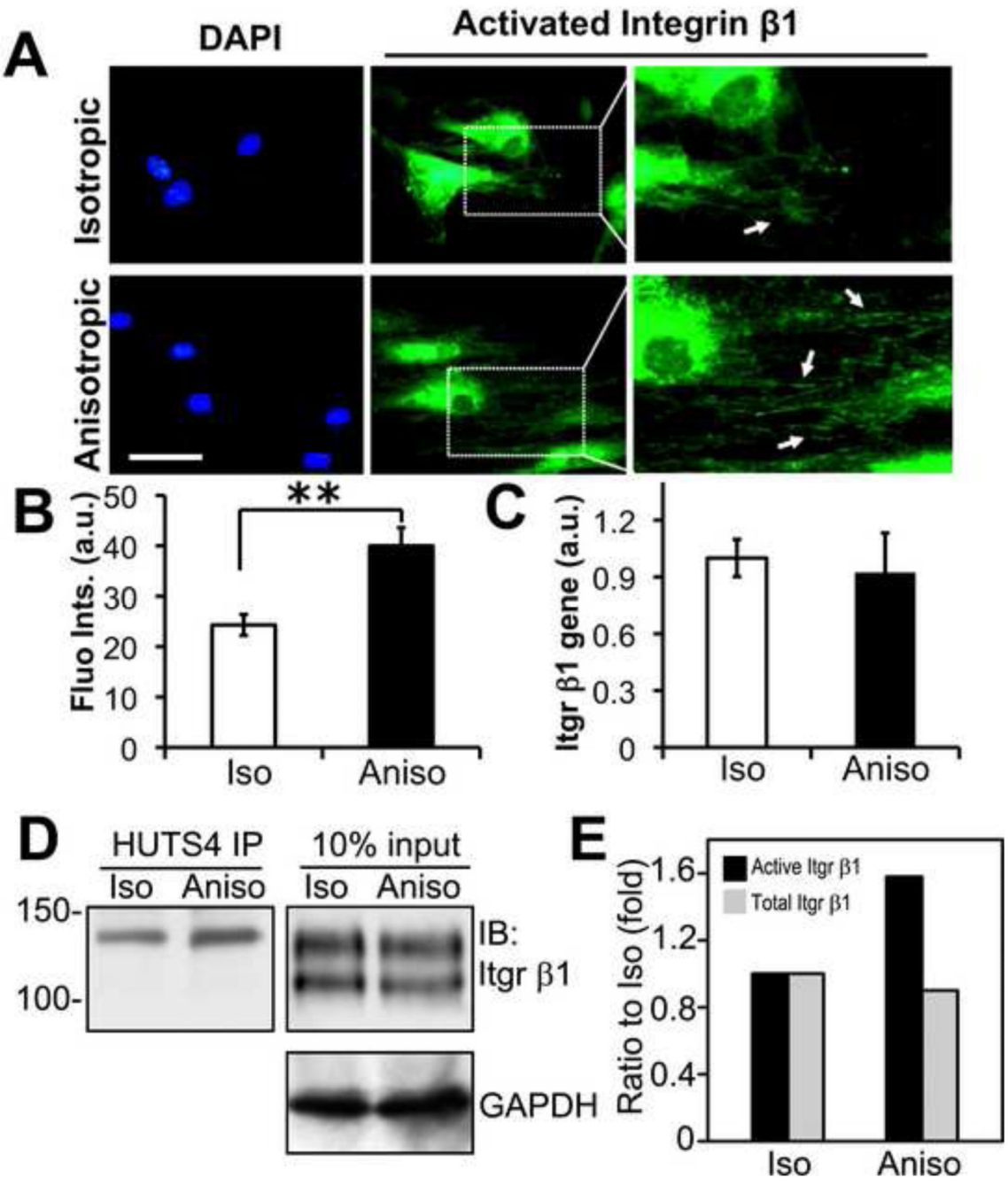

Figure 4.

PCL/Coll *anisotropic* nanofibrous matrix activates integrin β1 in human dermal fibroblasts. (A) Immunofluorescent staining of active integrin β1 on either *isotropic* or *anisotropic* matrices. White arrows indicate the distribution of active integrin β1. (B) Quantification of fluorescent intensity of active integrin β1 with a fluorometer. ** Statistically significant, $p < 0.01$. (C) Q-PCR analysis of integrinβ1 gene expression in *isotropic* and *anisotropic* groups. (D) Immunoprecipitation for active integrin β1. Cell lysates containing 1.5 mg proteins were immunoprecipitated with monoclonal antibody HUTS-4 that reacts with the activated epitope of human integrin β1. The immunoprecipitates and the input cell lysates were detected for the total integrin β1 by western blotting under non-reducing conditions.

GAPDH was used as a loading control. (E) Quantification of immunoblots. Integrin β1 immunoblots were quantified by densitometry and normalized against the loading control GAPDH. Integrin β1 activation was enhanced in cells cultured on *anisotropic* matrices (*Aniso*) compared to those on *isotropic* ones (*Iso*). Scale bar: 50μm.

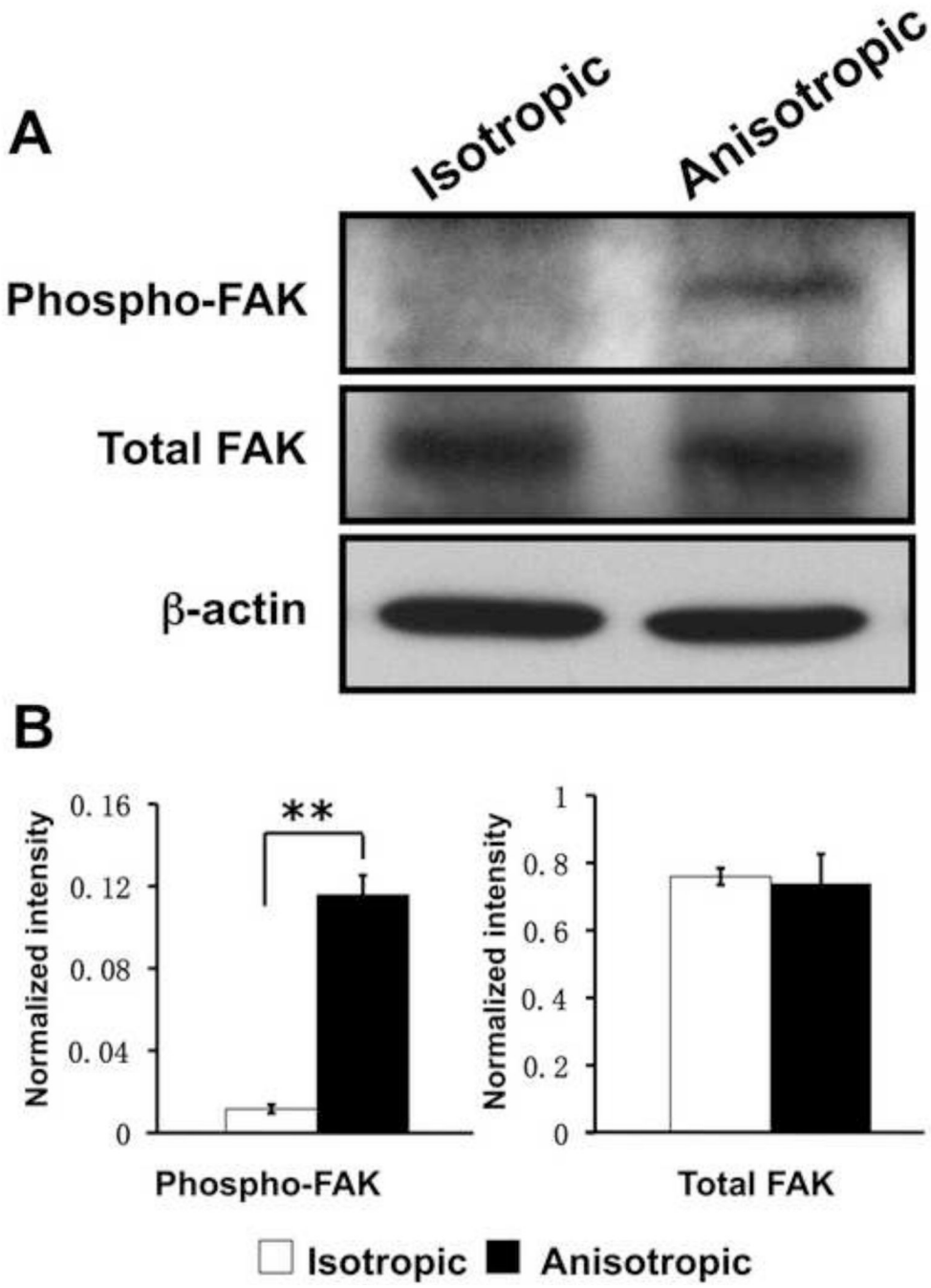

Figure 5.
Western blotting analysis of FAK phosphorylation (Tyr-397) in human dermal fibroblasts on PCL/Coll nanofibrous matrices. β-actin was used to normalize the protein input.

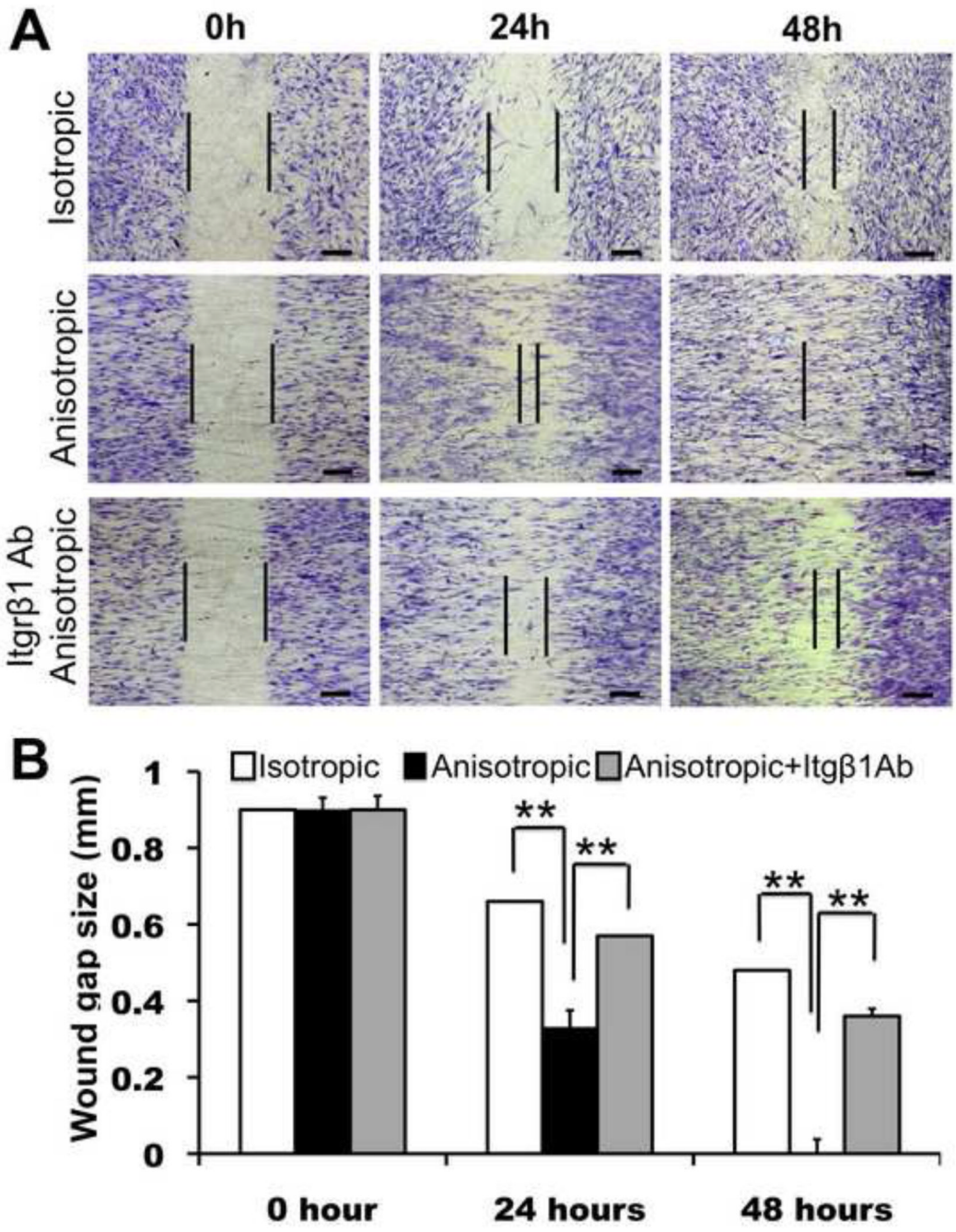

Figure 6.

Migration of human dermal fibroblasts on PCL/Coll nanofibrous matrices in wound healing assay. (A) Cells (5×10^4 per matrix) were seeded on either *isotropic* or *anisotropic* matrices with an insert in the middle. After 12 hours, the insert was removed to generate a 0.9-mm "wound gap". Cells were allowed to migrate into the wound gap, and visualized after 24 and 48 hours using methylene blue staining. (B) Quantification of the "wound gap" distance between the front lines of migrating fibroblasts (n=4). ** Statistically significant, p <0.01. Scale bar: 300μm

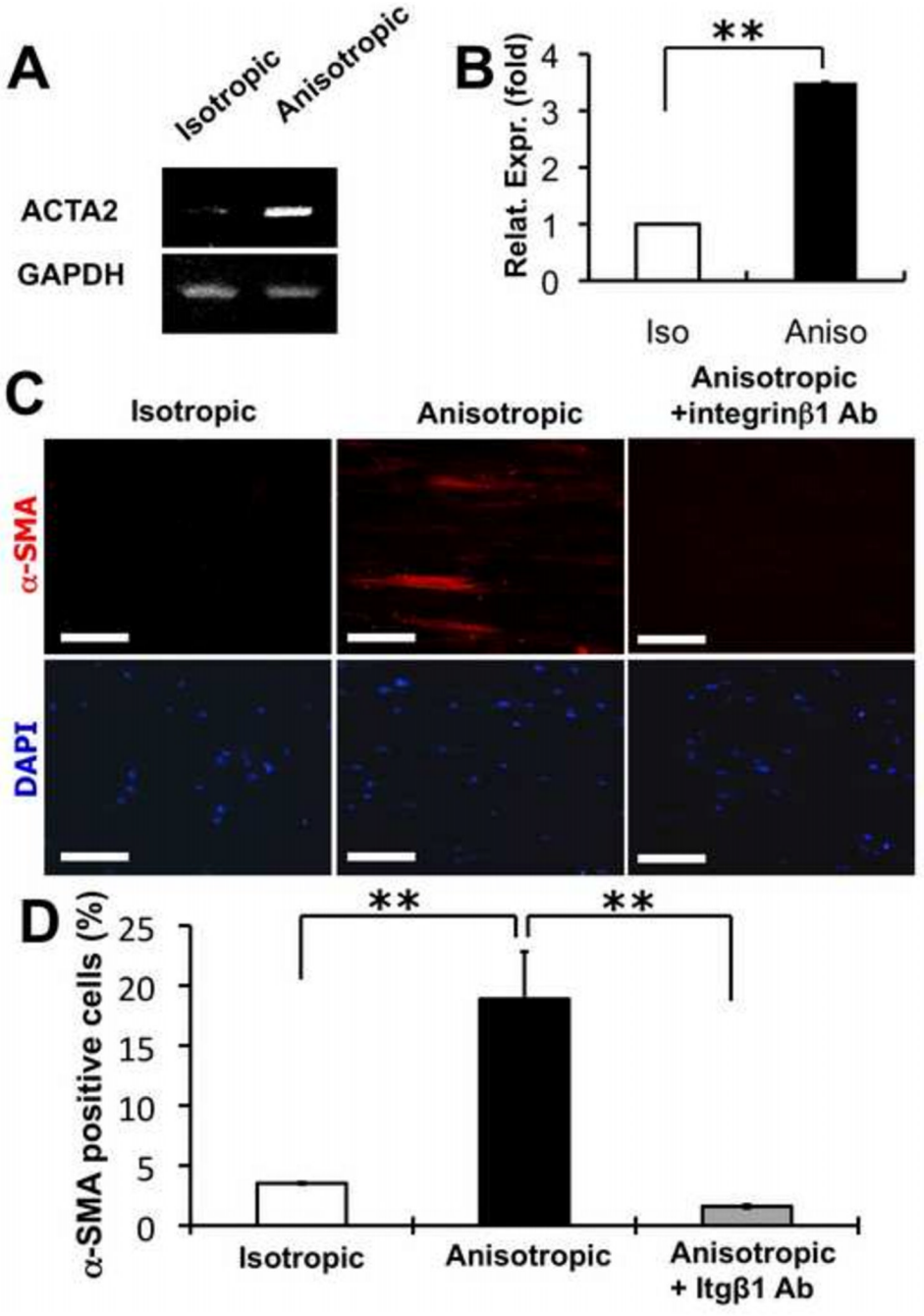

Figure 7.

Myofibroblastic differentiation of human dermal fibroblasts on PCL/Coll nanofibrous matrices. (A) RT-PCR and (B) Q-PCR analyses of cellular α-SMA (ACTA2) gene expression level on either *isotropic* or *anisotropic* nanofibrous matrices. (C) Immunostaining of cellular α-SMA proteins on *isotropic* and *anisotropic* matrices. (D) Quantification of α-SMA positive cells. The DAPI stained cell nuclei were used for normalization. ** Statistically significant, $p < 0.01$. Scale bar: 100 μm.

Table 1

Primers for various genes

Gene	Primer sequence
GAPDH	*Forward:* TGGATGGCCCCTCCGGGAAA
	Reverse: AGTGGGGACACGGAAGGCCA
3-actin	*Forward:* GAGGAATACAGCCTGTGGGT
	Reverse: CAGAAGGTGCAGAGATGATGA
ATCA2	*Forward:* CTTGGCTTGTCAGGGCTTGTCC
	Reverse: AGACCACTGCGCTCCACGTTGA
Integrin pi	*Forward:* GCTTTCTGTCACCTCTTCTAATCTTT
	Reverse: CGTAGGTGAGAGCTGTTGCATAG